Wu, Shili
107 Monticello
Piedmont, CA 94611
Tel: (510) 597-9140
Fax:(510) 601-6751

Thursday, August 29, 2002

Assistant Commissioner for Patents
Box Patent Application
Washington, DC 20231

Dear Ms or Mr.

My name is Shili Wu; I have engaged in research at Oklahoma Medical Research Foundation from Jan. 1997 until June 2002.

This week I found that there are obvious mistake of Inventors in two United States Patent Applications that I have made very important contribution. The details are as follows:

The First Patent Application is Catalytically active recombinant memapsin and methods of use thereof, the USPA #20020049303, Kind Code A1, Serial No.: 796264, Series Code 09, Filed: February 28 2001.

The Second Patent Application is Inhibitors of memapsin 2 and use thereof, the USPA #20020115600, Kind Code A1, Serial No.: 845226, Series Code: 09, Filed: April 30 2001.

I began research on Memapsin 2 in 1998 with Dr. Xinli Lin; at that time only our both worked on memapsin 2 research in Oklahoma Medical Research Foundation (OMRF). **Through more than one-year of hard work, by March 1999, I *first* got catalytically active recombinant memapsin 2 and had successfully refold memapsin 2 to obtain active enzyme in OMRF**. Without my hard work memapsin 2 may not have been found in OMRF.

After I got Memapsin 2, the whole department, which is headed by Dr. Jordan Tang, joins in on the research of Memapsin 2. By November 1999, the paper describing the results of research memapsin 2 was submitted to Proceedings of the National Academy of Sciences and was published in that journal in February 2000, with I as third author.

I have all original test notes that recorded all initial process of inventing Memapsin 2. They don't have the original test notes but a copy. I believe that they provided only copies to your office for reviewing.

In brief I made an important contribution to invent Memapsin 2, I am an initial inventor of Memapsin 2. My name should be in the above two US Patent Applications as one of the inventors.

So I claim that your office investigate the fact, find out the truth. I will keep further legal action right. Please feel free to contact me if you need further information about this matter.

Yours truly,

Shili Wu

Attachments:

1. Human aspartic protease memapsin 2 cleaves the β-secretase site of β-amyloid precursor protein; 1456-1460/ PNAS/February 15, 2000 / Vol.97/ No 4
2. Structure of the protease domain of memapsin 2 (β-Secretase) cpmplexed with inhibitor;
   SCIENCE / 6 October 2000/Volume 290/pp. 150-153

3. Unite States Patent Application 20020115600 web image database;
4. Unite States Patent Application 20020049303 web image database;

Human aspartic protease memapsin 2 cleaves the β-secretase site of β-amyloid precursor protein

Xinli Lin*, Gerald Koelsch*, Shili Wu*, Debbie Downs*, Azar Dashti*, and Jordan Tang*†‡

*Protein Studies Program, Oklahoma Medical Research Foundation, and †Department of Biochemistry and Molecular Biology, University of Oklahoma Health Sciences Center, Oklahoma City, OK 73104

Communicated by David R. Davies, National Institutes of Health, Bethesda, MD, December 14, 1999 (received for review November 2, 1999)

The cDNAs of two new human membrane-associated aspartic proteases, memapsin 1 and memapsin 2, have been cloned and sequenced. The deduced amino acid sequences show that each contains the typical *pre*, *pro*, and aspartic protease regions, but each also has a C-terminal extension of over 80 residues, which includes a single transmembrane domain and a C-terminal cytosolic domain. Memapsin 2 mRNA is abundant in human brain. The protease domain of memapsin 2 cDNA was expressed in *Escherichia coli* and was purified. Recombinant memapsin 2 specifically hydrolyzed peptides derived from the β-secretase site of both the wild-type and Swedish mutant β-amyloid precursor protein (APP) with over 60-fold increase of catalytic efficiency for the latter. Expression of APP and memapsin 2 in HeLa cells showed that memapsin 2 cleaved the β-secretase site of APP intracellularly. These and other results suggest that memapsin 2 fits all of the criteria of β-secretase, which catalyzes the rate-limiting step of the *in vivo* production of the β-amyloid (Aβ) peptide leading to the progression of Alzheimer's disease. Recombinant memapsin 2 also cleaved a peptide derived from the processing site of presenilin 1, albeit with poor kinetic efficiency. Alignment of cleavage site sequences of peptides indicates that the specificity of memapsin 2 resides mainly at the S_1' subsite, which prefers small side chains such as Ala, Ser, and Asp.

membrane aspartic proteases | Alzheimer's disease

Many proteases are intimately involved in the regulation of cellular and physiological functions. There are five well studied human aspartic proteases. Pepsin and gastricsin participate in digestion in the stomach whereas cathepsins D and E function in intracellular protein degradation in lysosomes and endosomes. Human cathepsin D has been implicated in the metastasis of breast cancer and in Alzheimer's disease. Renin catalyzes the conversion of angiotensinogen to angiotensin 1, a clinically important step in hemostasis. The intimate involvement of human aspartic proteases in physiology and disease illustrates their central role in biology and medicine.

The emergence of human gene sequences in the expressed sequence tag (EST) database represents an important new resource for identifying novel human enzymes. We report here the cloning of two new human aspartic proteases, memapsin 1 (M1) and memapsin 2 (M2), initially identified from the human EST database. These proteases are unique among aspartic proteases in that they are membrane-anchored. The presence of M2 in the brain led us to test its capacity to hydrolyze the β-amyloid precursor protein (APP). Detailed enzymic and cellular studies suggest that M2 fits all of the criteria of β-secretase. Like M2, APP is a type I integral transmembrane protein and is known to be processed *in vivo* at three sites. The evidence suggests that cleavage at the α-secretase site by a membrane-associated metalloprotease is a physiological event. This site is located in APP 12 residues away from the luminal surface of the plasma membrane. Cleavage of the β-secretase site (28 residues from the plasma membrane's luminal surface) and the γ-secretase site (in the transmembrane region) results in a 40/42-residue β-amyloid peptide (Aβ), whose elevated production and accumulation in the brain are the central events in the pathogenesis of Alzheimer's disease (for review, see ref. 1). Presenilin 1, another membrane protein found in human brain, controls the hydrolysis at the APP γ-secretase site and has been postulated to be itself the responsible protease (2). Presenilin 1 is expressed as a single chain molecule, and its processing by a protease, presenilinase, is required to prevent it from rapid degradation (3, 4). The identity of presenilinase is unknown. The *in vivo* processing of the β-secretase site is thought to be the rate-limiting step in Aβ production (5) and, thus, is a strong therapeutic target. The production of recombinant M2 in *Escherichia coli* and the information on its specificity reported here should be useful for the design and testing of potential inhibitor drugs.

Materials and Methods

Cloning of Memapsin 2. Three new EST sequences homologous to human aspartic proteases were found in EST database (www.ncbi.nlm.nih.gov) (EST AA136368, from human pregnant uterus; EST AA207232, from human neurepithelium; EST R55398, from human breast) using human aspartic protease motifs as a query. The corresponding bacterial strains 947471, 214526, and 392689 containing the EST sequences were obtained from the American Type Culture Collection. The completed sequences from these clones assembled into ≈80% of *prepro*-M2 cDNA. The 5′ region of M2 cDNA was obtained by using 5′ rapid amplification of cDNA ends PCR, which was carried out by using human pancreas Marathon-Ready cDNA (CLONTECH) and human pancreatic λ-gt10 and λ-gt11 libraries as templates and M2 specific primers. *Prepro*-M1 cDNA was cloned by using a similar procedure.

Tissue Distribution of Memapsin 1 and 2 mRNA. Multiple human tissue cDNA panels (CLONTECH) were used as template for PCR amplification (30 cycles) of a 0.56-kb memapsin 1 cDNA fragment using primers M1F1 (5′-GACGTCACATGTAAGTACACACAAGGAAGC) and M1R2 (5′-CAGAGATGCGCGGGCCACAGCTTCCACCAC), and of a 0.82-kb memapsin 2 cDNA fragment using primers M2F1 (5′-GGTAAGCATCCCCCATGGCCCCAACGTC-3′) and M2R2 (5′-CCAATTCGTTTTCGGGCCCGATCAAAGACAACG-3′). The amplified fragments were compared in agarose gel electrophoresis.

***E. coli* Expression of the Protease Domain of *pro*-Memapsin 2.** A fragment of M2 cDNA encoding the estimated *pro* and protease domain (without the C-terminal extension) were PCR amplified

Abbreviations: APP, β-amyloid precursor protein; M1, memapsin 1; M2, memapsin 2; EST, expressed sequence tag.

Data deposition: The sequences reported in this paper have been deposited in the GenBank database [accession nos. AF200192 (memapsin 1) and AF200193 (memapsin 2)].

‡To whom reprint requests should be addressed at: Protein Studies Program, Oklahoma Medical Research Foundation, 825 NE 13 Street, Oklahoma City, OK 73104. E-mail: jordan-tang@omrf.ouhsc.edu.

The publication costs of this article were defrayed in part by page charge payment. This article must therefore be hereby marked "*advertisement*" in accordance with 18 U.S.C. §1734 solely to indicate this fact.

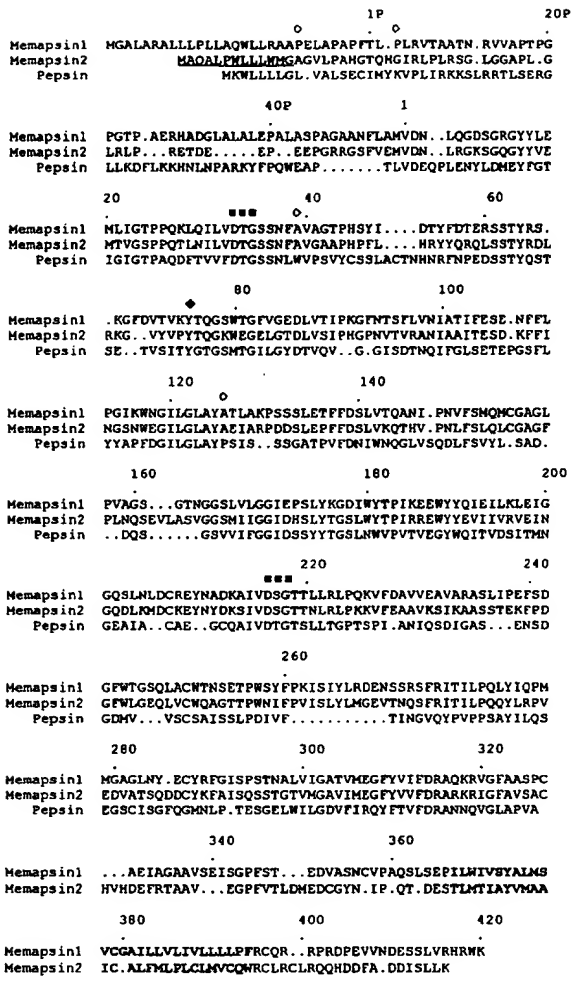

Fig. 1. Predicted amino acid sequence of human *prepro*-memapsin 1 (GenBank accession no. AF200192) and *prepro*-memapsin 2 (GenBank accession no. AF200193) aligned against the sequence of human *pre*-pepsinogen. Amino acid codes are according to standard International Union of Pure and Applied Chemistry nomenclature. The beginning of *pro* and mature protease regions of pepsinogen are marked by residue numbers 1P and 1, respectively. Two active-site aspartic acids in D(T/S)G motifs are marked by ■ and conserved Tyr^{75} by ◆. Residues in the predicted transmembrane domains are in boldface.

and inserted into the *Bam*HI site of vector pET11a. The resulting vector, pET11-$PM2_{pd}$, expresses a protein, *pro*-$M2_{pd}$, whose sequence starts from Ala^{-8P} to Ala^{326} [pepsin residue numbering (Fig. 1)]. The expression and purification of $M2_{pd}$ was carried out in *E. coli* strain BL21(DE3) as previously described (6) with minor modifications as follows: inclusion bodies dissolved in 8 M urea were rapid-diluted into 20 mM Tris base, and the pH was adjusted to 8.0.

Activation of *pro*-Memapsin 2 and Enzyme Kinetics. Incubation in 0.1 M sodium acetate (pH 4.0) for 16 h at 22°C autocatalytically converted *pro*-$M2_{pd}$ to $M2_{pd}$. For initial hydrolysis tests, two synthetic peptides were separately incubated with *pro*-$M2_{pd}$ in 0.1 M Na acetate (pH 4.0) for different periods ranging from 2 to 18 h. The incubated samples were subjected to HPLC/mass spectroscopy for the identification of the hydrolytic products (average error in mass determination was 0.02%). For kinetic studies, the identified HPLC (Beckman System Gold) product peaks were integrated for quantitation. The K_m and k_{cat} values for presenilin 1 and Swedish-APP peptides (Table 1) were

Table 1. Alignment on amino acids appearing in eight subsites of memapsin substrates

	Subsites							
Peptide	P4	P3	P2	P1	P1′	P2′	P3′	P4′
APP β	E	V	K	M	D	A	E	F
Swedish APP β	E	V	N	L	D	A	E	F
PS-1	L	V	N	M	A	E	G	D
M2-Pro	R	G	S	M	A	G	V	L
	G	T	Q	H	G	I	R	L
M2	S	S	N	F	A	V	G	A
	G	L	A	Y	A	E	I	A
Insulin B-chain	H	L	C*	G	S	H	L	V
	C*	G	E	R	G	F	F	Y
	E	A	L	Y	L	V	C*	G
Nch†	G	V	L	L	S	R	K	
		V	G	S	G	V	L	L
				V	G	S	G	V

*C is cysteic acid.
†Nch sequence VGSGVLLSRK.

measured by steady-state kinetics. The individual K_m and k_{cat} values for APP peptide could not be measured accurately by standard methods, so its k_{cat}/K_m value was measured by competitive hydrolysis of mixed substrates against presenilin 1 peptide (7).

Mammalian Cell Transfections. *Pro*-M2 cDNA was cloned into the *Eco*RV site of vector pSecTag A (Invitrogen). Human APP cDNA was PCR amplified from human placenta λ-gt11 library (CLONTECH) and was cloned into the *Nhe*I and *Xba*I sites of pSecTag A. The procedure for transfection into HeLa cells and vaccinia virus infection for T7-based expression are essentially the same as described (8).

Pulse–Chase and Immunodetection. Transfected cells were metabolically labeled with 200 μCi of ^{35}S methionine and cysteine (TransLabel; ICN) in 0.5 ml of serum-free/methionine-free media for 30 min, were rinsed with 1 ml of media, and were replaced with 2 ml of DMEM/10% FCS. To block vesicle acidification, bafilomycin A1 was included in the media (9). At different time points (chase), media was removed and the cells were harvested and lysed in 50 mM Tris, 0.3 M NaCl, 5 mM EDTA, and 1% Triton X-100 (pH 7.4) containing 10 mM iodoacetamide, 10 μM TPCK, 10 μM TLCK, and 2 μg/ml leupeptin. The supernatant (14,000 × *g*) of cell lysates and media were immunoadsorbed onto antibody bound to protein G Sepharose (Sigma). Anti-APP N-terminal domain antibody (Chemicon) was used to recover the Nβ-fragment of APP, and anti-$A\beta_{1-17}$ antibody (Chemicon, recognizing the N-terminal 17 residues of Aβ) was used to recover the 12 kDa βC-fragment. The former antibody recognized only denatured protein, so media was first incubated in 2 mM dithiothrietol and 0.1% SDS at 55°C for 30 min before immunoadsorption. Samples were cooled and diluted with an equal volume of cell lysis buffer before addition of anti-APP N-terminal domain (Chemicon). Beads were washed, were eluted with loading buffer, were subjected to SDS/PAGE (NOVEX, San Diego), and were visualized by autoradiogram or PhosphorImaging (Molecular Dynamics) on gels enhanced with Amplify (Amersham). Immunodetection of the Nα fragment was accomplished by transblotting onto a PVDF membrane and detecting with anti-$A\beta_{1-17}$ and chemiluminescent substrate (Amersham).

Cellular Localization of M2 and APP. HeLa cells transfected with APP or M2 (see above) in four-well chamber slides were fixed

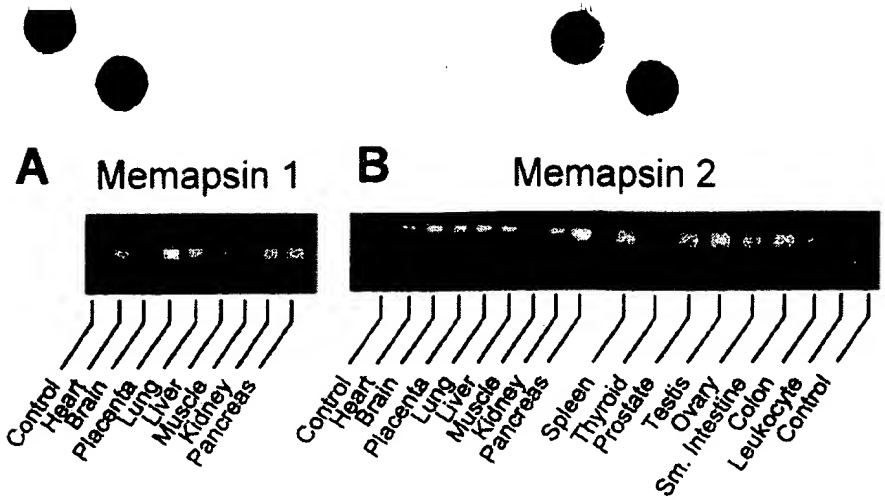

Fig. 2. Tissue distribution of M1 (*A*) and M2 (*B*) mRNA determined by reverse transcription–PCR visualized in agarose gel electrophoresis. Control experiment contained no template DNA. Amplification of glyceraldehyde-3-phosphate dehydrogenase mRNA produced uniform intensity (data not shown).

with acetone for 10 min and were permeabilized in 0.2% Triton X-100 in PBS for 6 min. For localizing M2, polyclonal goat anti-*pro*-$M2_{pd}$ antibodies were purified on DEAE-Sepharose 6B and were affinity-purified against recombinant *pro*-$M2_{pd}$ immobilized on Affigel (Bio-Rad). Purified anti-*pro*-$M2_{pd}$ antibodies were conjugated to Alexa568 (Molecular Probes) according to the manufacturer's protocol. Fixed cells were incubated overnight with a 1:100 dilution of antibody in PBS containing 0.1% BSA and were washed four times with PBS. For APP, two antibodies were used: antibody $A\beta_{1-17}$ (described above) and antibody $A\beta_{17-42}$, which recognizes the first 26 residues after the α-secretase cleavage site (Chemicon). After four PBS washes, the cells were incubated overnight with an anti-mouse FITC conjugate at a dilution of 1:200. Cells were mounted in Prolong anti-fade reagent (Molecular Probes) and were visualized on a Leica (Deerfield, IL) TCS confocal laser scanning microscope.

Results

EST clones from three human cDNAs were identified from homology search based on aspartic protease motifs and were sequenced after 5′ rapid amplification of cDNA ends. The deduced protein sequences (Fig. 1) are characteristic of mammalian aspartic protease zymogens. Uniquely, each enzyme also has a C-terminal extension of over 80 residues (see Fig. 1 alignment with pepsin), which includes a putative transmembrane region. The enzymes are named memapsin 1 and memapsin 2 (for membrane-anchored aspartic protease of the pepsin family; GenBank accession nos. AF200192 and AF200193, respectively). In human tissues, spleen and prostate have the highest levels of M1 mRNA level [but is absent in the brain (Fig. 2*A*)] whereas pancreas and brain have the highest amount of M2 (Fig. 2*B*). To search for M2 substrates among membrane proteins of the brain, the estimated *pro*-M2 protease domain (*pro*-$M2_{pd}$, without the C-terminal extension) was expressed in *E. coli* as inclusion bodies, refolded and purified. In acidic solutions, *pro*-$M2_{pd}$ spontaneously generated activity (see below) with the concomitant appearance of smaller fragments (Fig. 1, Fig. 3*A*, and Table 1), a common property for aspartic protease zymogens. Whether this activity is produced by the classical intramolecular activation of aspartic protease zymogens (10, 11) is presently unknown. For the current discussion, we will refer to this activity as that of M2 ($M2_{pd}$).

Modeling of M2 three-dimensional structure as a type I integral membrane protein suggested that its globular protease unit can hydrolyze a membrane-anchored polypeptide at a distance range of 20–30 residues from the membrane surface (results not shown). As a transmembrane protein of the brain, APP is a potential substrate. Its β-secretase site, located about 28 residues from the plasma membrane surface, is within in the range for M2 proteolysis. A synthetic peptide derived from this site (SEVKM/DAEFR) was hydrolyzed by $M2_{pd}$ at the β-secretase site (marked by a slash). A second peptide (SEVNL/DAEFR) derived from APP β-secretase site with the "Swedish mutation" (12), known to elevate the level of Aβ production in cells (13), was hydrolyzed by $M2_{pd}$ with much higher catalytic efficiency (Fig. 3*C*). Both substrates were optimally cleaved at pH 4.0 (Fig. 3*B*). A peptide derived from the processing site of presenilin 1 (SVNM/AEGD) was also cleaved by $M2_{pd}$ with poor kinetic parameters (Fig. 3*C*). A peptide derived from the APP γ-secretase site (KGGVVIATVIVK) was not cleaved by $M2_{pd}$. Interestingly, pepstatin A inhibited $M2_{pd}$ poorly ($IC_{50} \approx 0.3$ mM). The kinetic parameters indicate that both presenilin 1 (k_{cat}, 0.67 s^{-1}; K_m, 15.2 mM; k_{cat}/K_m, 43.8 $s^{-1}\cdot M^{-1}$) and native APP peptides (k_{cat}/K_m, 39.9 $s^{-1}\cdot M^{-1}$) are very poor substrates whereas Swedish APP peptide (k_{cat}, 2.45 s^{-1}; K_m, 1 mM; k_{cat}/K_m, 2,450 $s^{-1}\cdot M^{-1}$) is a much better substrate.

To determine whether M2 possesses an APP β-secretase function in mammalian cells, these two cDNAs were transiently expressed in HeLa cells (8), were metabolically pulse-labeled with ^{35}S-Met, and then were immunoprecipitated with anti-APP antibodies for visualization of APP-generated fragments after SDS/polyacrylamide electrophoresis and imaging. Cells expressing both APP and M2 produced the 97-kDa APP Nβ-

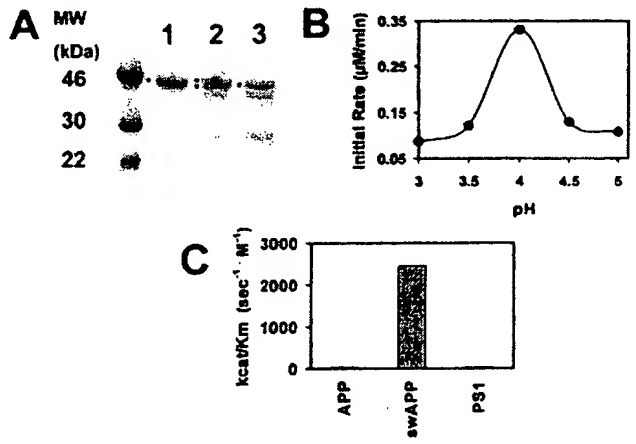

Fig. 3. (*A*) Conversion of *pro*-$M2_{pd}$ (lane 1) at pH 4.0 to smaller fragments (lane 3) as shown by SDS/polyacrylamide electrophoretic pattern. Difference in migration between *pro*-$M2_{pd}$ and converted enzyme is evident in a mixture of the two (lane 2). Squares mark band positions. (*B*) Initial rate of hydrolysis of synthetic peptide swAPP (see Table 1) by $M2_{pd}$ at different pH. (*C*) Relative k_{cat}/K_m values for steady-state kinetic of hydrolysis of peptide substrates by $M2_{pd}$ (see text for peptides and values).

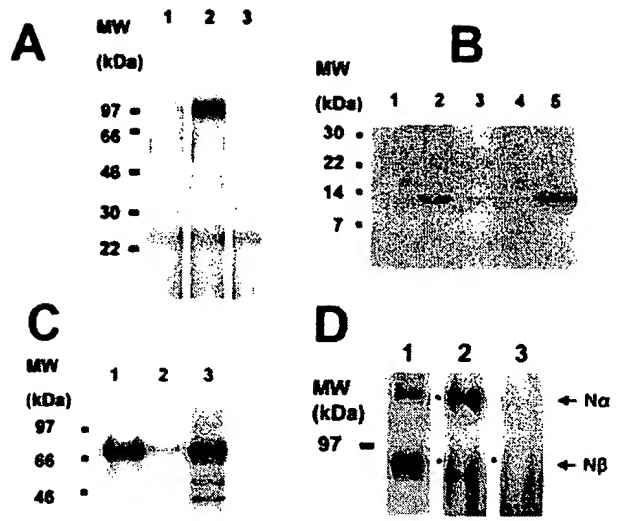

Fig. 4. Processing of APP by M2 in HeLa cells. (*A*) SDS/PAGE patterns of immunoprecipitated APP Nβ-fragment (97-kDa band) from the condition media (2 h) of pulse–chase experiments. Lanes: 1, transfection of APP alone; 2, co-transfection of APP and M2; 3, same as lane 2 except that bafilomycin A1 is included. (*B*) SDS/PAGE patterns of APP βC-fragment (12 kDa) immunoprecipitated from the conditioned media of the same experiment as in *A*. Lanes: 1, transfection of APP; 2, co-transfection of APP and M2; 3, as in lane 2 but with bafilomycin A1; 4, transfection of Swedish APP; 5, co-transfection of Swedish APP and M2. (*C*) SDS/PAGE patterns of immunoprecipitated M2 (70 kDa). Lanes: 1, M2 transfected cells; 2, untransfected HeLa cells after long time film exposure; 3, endogenous M2 from HEK 293 cells. (*D*) SDS/PAGE patterns of APP fragments (100-kDa Nα-fragment and 95-kDa Nβ-fragment) recovered from conditioned media after immunoprecipitation using antibodies specific for the N-terminal region of APP. Lanes: 1, autoradiogram of immunoprecipitation from co-transfection of APP and M2; 2 and 3, immunoblotted by using antibody Aβ_{1-17}, specific for the Nα-fragment that does not recognize the Nβ-fragment; 2, transfection with APP alone; 3, co-transfection of APP and M2. Dots mark band positions.

fragment (from the N terminus to the β-secretase site) in the conditioned media (Fig. 4*A*, lane 2) and the 12-kDa βC-fragment (from the β-secretase site to the C terminus) in the cell lysate (Fig. 4*B*, lane 2). Controls that included transfection of APP alone produced little detectable Nβ-fragment (Fig. 4*A*, lane 1) nor the βC-fragment (Fig. 4*B*, lane 1). Bafilomycin A1, which is known to raise the intravesicle pH of lysosomes/endosomes and has been shown to inhibit APP cleavage by β-secretase (14), abolished the production of both APP fragments Nβ and βC (Fig. 4*A*, lane 3 and Fig. 4*B*, lane 3, respectively) in co-transfected cells. Transfection of cells with Swedish APP alone did not produce the βC-fragment band in the cell lysate (Fig. 4*B*, lane 4), but the co-transfection of Swedish APP and M2 did (Fig. 4*B*, lane 5). This Swedish βC-fragment band is more intense than that of the wild-type APP (Fig. 4*B*, lane 2). A 97-kDa Nβ-band is also seen in the conditioned media but is about the equal intensity as the wild-type APP transfection (result not shown). These results suggest that M2 processes the β-secretase site of APP in acidic compartments such as the endosomes. To establish the expression of transfected M2 gene, the pulse-labeled cells were lysed and immunoprecipitated by anti-M2 antibodies. A 70-kDa M2 band was seen in cells transfected with M2 gene (Fig. 4*C*, lane 1), which has the same mobility as the major band from HEK 293 cells (Fig. 4*C*, lane 3) known to express β-secretase (13). A very faint band of M2 is also seen, after a long film exposure, in untransfected HeLa cells (Fig. 4*C*, lane 2), indicating a very low level of endogenous M2, which was insufficient to produce Nβ- or βC-fragments without M2 transfection (Fig. 4*A*, lane 1 and Fig. 4*B*, lane 1). Antibody Aβ_{1-17}, which specifically

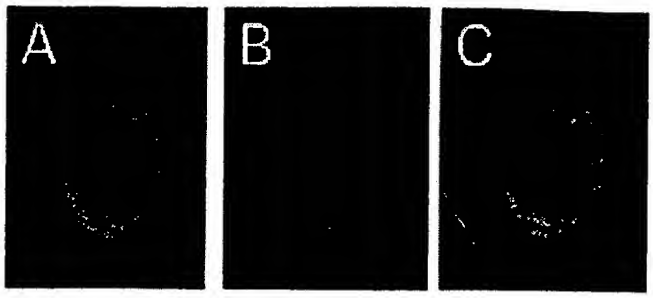

Fig. 5. Intracellular localization of M2 and APP in a single cell. HeLa cells co-expressing APP and M2 were stained with antibodies directed toward APP (*A*, green image) and M2 (*B*, red image) and were visualized simultaneously by CSLM (see *Materials and Methods*) using a 100× objective. Areas of colocalization appear in yellow in overlay of two images in *C*.

recognizes residues 1–17 in Aβ peptide, was used to confirm the correct β-secretase site cleavage. From immunoprecipitation of conditioned media from cells transfected with APP and M2, both Nα- and Nβ-fragments are visible using an antibody recognizing the N-terminal region of APP present in both fragments (Fig. 4*C*, lane 1). In Western blots, antibody Aβ_{1-17} recognized the immunoprecipitated Nα-fragment produced by endogenous α-secretase in the untransfected cells (Fig. 4*C*, lane 2). This antibody was, however, unable to recognize the Nβ-fragment (Fig. 4*C*, lane 3) known to be present in cells co-transfected with APP and M2 (compare the 95-kDa band in lanes 1 and 3). These observations confirmed that Nβ-fragment is the product of β-secretase site cut by M2, which abolished recognition of the epitope of Aβ_{1-17}.

The processing of APP by M2 predicts the intracellular colocalization of the two proteins. Immunodetection observed by confocal microscopy of both APP (Fig. 5*A*) and M2 (Fig. 5*B*) revealed their colocalization in the superimposed scans (Fig. 5*C*). The distribution of both proteins is consistent with their residence in lysosomal/endosomal compartments.

In specificity studies, we found that $M2_{pd}$ cleaved its *pro* peptide (two sites) and the protease portion (two sites) during a 16-h incubation after activation (Table 1). Besides the three peptides discussed above, $M2_{pd}$ also cleaved oxidized bovine insulin B chain and a synthetic peptide Nch. Interestingly, we found that native proteins were not cleaved by $M2_{pd}$ (including β-amylase, alcohol dehydrogenase, carbonic anhydrase, cytochrome C, bovine and human serum albumin, hemoglobin, and chicken egg lysozyme; data not shown). The residues around all of these cleavage sites are aligned in Table 1. The specificity of M2 derived from these results will be further discussed below.

Discussion

The data presented herein strongly suggest that human M2 fulfills all of the criteria of a β-secretase that cleaves the β-amyloid precursor protein (APP): (*i*) M2 and APP are both membrane proteins present in human brain and co-localize in mammalian cells, (*ii*) M2 specifically cleaves the β-secretase site of synthetic peptides and of APP in cells, (*iii*) M2 preferentially cleaves the β-secretase site from the Swedish over the wild-type APP, and (*iv*) the acidic pH optimum for M2 activity and bafilomycin A1 inhibition of APP processing by M2 in the cells are consistent with the previous observations that β-secretase cleavage occurs in acidic vesicles (14). The spontaneous appearance of activity of recombinant pro-M2 in an acidic solutions is consistent with the idea that this zymogen can by itself generate activity in an acidic vesicle like an endosome. However, we note that the cleavage sites (Table 1) are not near the vicinity of the aligned pepsin N terminus (Fig. 1). It seems probable that the activation of proM2 *in vivo* may require another protease. While

preparing this manuscript, the cloning of a human transmembrane aspartic protease BACE and its activity in the cleavage of APP β-secretase site were reported (15). The sequences of BACE and *pro*-memapsin 2 are identical. Although the approaches used for cloning, transfection, and expression were different in these two studies, both studies concluded that the new protease is β-secretase, the long-sought enzyme inexorably involved in Alzheimer's disease.

We have determined that the hydrolysis of the Swedish peptide by $M2_{pd}$ has a k_{cat}/K_m value $\approx 60\times$ over that for the wild-type APP peptide, which explains the higher production of Aβ peptide and the early onset of Swedish familial Alzheimer's disease (12). The relative amount of β-secretase cleavage of APP and Swedish APP estimated from the cellular experiments is only about six-fold in favor of Swedish APP (13). We also observed only a few-fold increase of the βC-fragment from Swedish APP over that of native APP (Fig. 4*B*). Although β-secretase is known to be the rate-limiting step in the production of Aβ peptide from native APP (5), the cellular processing of Swedish APP, with $60\times$ of catalytic efficiency, would likely make other steps in Aβ production to be rate limiting. The correct cleavage of a peptide from the processing site of presenilin 1 by $M2_{pd}$ (Table 1) could be taken to suggest that M2 may be the presenilin 1 processing protease, presenilinase. This seems to be improbable because the kinetics are not sufficiently robust for the required physiological efficiency. There may also be a question of accessibility of the presenilinase site by M2 that is located on the luminal side of the membrane. Evidence for the localization of the processing loop of presenilin 1 on the luminal (16) and cytosolic (17) sides of the membrane have both been reported.

Data presented in Table 1 suggest that M2 has an overall broad substrate specificity. Among the eight subsites, present in all aspartic proteases, the most stringent specificity for M2 occurs at S_1', which prefers small or negatively charged side chains, such as Ala, Asp, and Ser, or no side chain, Gly. Our data on the P_1 preference are in general agreement but somewhat broader than the results of a cellular mutagenesis study (18) in which Tyr, Leu, Phe, and Met were found at P_1. This is expected from a higher sensitivity for product detection in our experiments. Other subsites show relatively high tolerance for side chains of different sizes and charges. From the sequences of the peptide substrates that were cleaved, there appears to be a trend of requiring at least two large hydrophobic residues in these eight subsites. These specificity findings suggest that the P_1/P_1' residues at the α-secretase site (Lys/Leu) and the γ-secretase site (Val/Ile and Ala/Thr) are not favored by M2 and would predict that they are not substrates. The failure of M2 to cleave native proteins is consistent with the requirement in a substrate of a stretch of peptide in an extended conformation. The hydrolysis of Nch peptide between residues 1–2 and 3–4 (Table 1) suggests that the hydrolysis by M2 does not require a substrate to fill all eight substrate binding subsites. This may indicate that a relatively short peptidic transition-state analogue can be a good inhibitor for M2.

Even though the molecular architecture of the two memapsins are similar, because M1 is absent in the brain (Fig. 2*A*), the question as to whether it can cleave the APP β-secretase site may be physiologically irrelevant. However, the presence of both M1 and M2 in many other tissues argues for important roles of this new class of aspartic proteases in other physiological processes. The poor kinetic parameters for the hydrolysis of β-secretase site of native APP by M2 suggest that this cleavage may be a tolerated aberration in normal human brain.

The authors thank Dr. J. Donald Capra (Oklahoma Medical Research Foundation) for critical reading of the manuscript, Dr. Ken Jackson, Jihua Wang, and Jim Henthorn of the Warren Medical Research Foundation, University of Oklahoma Health Sciences Center, for assistance in mass spectrometry and confocal microscopy, and Dr. David Powell (SmithKline Beecham Pharmaceuticals) for helpful discussion. G.K. is a Scientist Development Awardee of the American Heart Association (9930115N). J.T. is holder of the J. G. Puterbaugh Chair in Biomedical Research at the Oklahoma Medical Research Foundation.

1. Selkoe, D. J. (1999) *Nature (London)* **399A,** 23–31.
2. Wolfe, M. S., Xia, W., Ostaszewski, B. L., Diehl, T. S., Kimberly, W. T. & Selkoe, D. J. (1999) *Nature (London)* **398,** 513–517.
3. Thinakaran, G., Borchelt, D. R., Lee, M. K., Slunt, H. H., Spitzer, L., Kim, G., Ratovitsky, T., Davenport, F., Nordstedt, C., Seeger, M., *et al.* (1996) *Neuron* **17,** 181–190.
4. Podlisny, M. B., Citron, M., Amarante, P., Sherrington, R., Xia, W., Zhang, J., Diehl, T., Levesque, G., Fraser, P., Haass, C. *et al.* (1997) *Neurobiol. Dis.* **3,** 325–337.
5. Sinha, S. & Lieberburg, I. (1999) *Proc. Natl. Acad. Sci. USA* **96,** 11049–11053.
6. Lin, X., Lin, Y. & Tang, J. (1994) *Methods Enzymol.* **241,** 195–224.
7. Fersht, A. (1985) *Enzyme Structure and Mechanism* (Freeman, New York).
8. Lin, X., Dashti, A., Schinazi, R. F. & Tang, J. (1993) *FASEB J.* **7,** 1070–1080.
9. Perez, R. G., Squazzo, S. L. & Koo, E. H. (1996) *J. Biol. Chem.* **271,** 9100–9107.
10. Tang, J. & Wong, R. N. S. (1987) *J. Cell. Biochem.* **33,** 53–63.
11. Koelsch, G., Loy, J., Lin, X. & Tang, J. (1998) *Adv. Exp. Med. Biol.* **436,** 245–252.
12. Mullan, M., Houlden, H., Windelspecht, M., Fidani, L., Lombardi, C., Diaz, P., Rossor, M., Crook, R., Hardy, J., Duff, K., *et al.* (1992) *Nat. Genet.* **2,** 340–342.
13. Citron, M., Oltersdorf, T., Haass, C., McConlogue, L., Hung, A. Y., Seubert, P., Vigo-Pelfrey, C., Lieberburg, I. & Selkoe, D. J. (1992) *Nature (London)* **260,** 672–674.
14. Knops, J., Suomensaari, S., Lee, M., McConlogue, L., Serbert, P. & Sinha, S. (1995) *J. Biol. Chem.* **270,** 2419–2422.
15. Vassar, R., Bennett, B. D., Babu-Khan, S., Kahn, S., Mendiaz, E. A., Denis, P., Teplow, D. B., Ross, S., Amarante, P., Loeloff, R. *et al.* (1999) *Science* **286,** 735–741.
16. Dewji, N. N. & Singer, S. J. (1997) *Proc. Natl. Acad. Sci. USA* **94,** 1425–1430.
17. De Strooper, B., Beullens, M., Contreras, B., Levesque, L., Craessaerts, K., Cordell, B., Moechars, D., Bollen, M., Fraser, P., George-Hyslop, P. S. *et al.* (1997) *J. Biol. Chem.* **272,** 3590–3598.
18. Citron, M., Taplow, D. B. & Selkoe, D. J. (1995) *Neuron* **14,** 661–670.

Structure of the Protease Domain of Memapsin 2 (β-Secretase) Complexed with Inhibitor

Lin Hong,[1] Gerald Koelsch,[1] Xinli Lin,[1] Shili Wu,[1] Simon Terzyan,[2] Arun K. Ghosh,[3] Xuenjun C. Zhang,[2] Jordan Tang[1,4*]

Memapsin 2 (β-secretase) is a membrane-associated aspartic protease involved in the production of β-amyloid peptide in Alzheimer's disease and is a major target for drug design. We determined the crystal structure of the protease domain of human memapsin 2 complexed to an eight-residue inhibitor at 1.9 angstrom resolution. The active site of memapsin 2 is more open and less hydrophobic than that of other human aspartic proteases. The subsite locations from S_4 to S_2' are well defined. A kink of the inhibitor chain at P_2' and the change of chain direction of P_3' and P_4' may be mimicked to provide inhibitor selectivity.

The accumulation of the 40- to 42-residue β-amyloid peptide (Aβ) in the brain is a key event in the pathogenesis of Alzheimer's disease (AD) (*1*). Aβ is generated in vivo through proteolytic cleavage of the membrane-anchored β-amyloid precursor protein (APP) by β- and γ-secretases. The γ-secretase activity, which cleaves APP within its transmembrane domain, is likely mediated by the transmembrane protein presenilin 1 (*2–4*). The β-secretase cleaves APP on the lumenal side of the membrane and its activity is the rate-limiting step of Aβ production in vivo (*5*). Both proteases are potential targets for inhibitor drugs against AD. Our group (*6*) and others (*7*) recently cloned a human brain aspartic protease, memapsin 2 or BACE, and demonstrated it to be β-secretase. Memapsin

[1]Protein Studies Program and [2]Crystallography Program, Oklahoma Medical Research Foundation, 825 NE 13th Street, Oklahoma City, OK 73104, USA. [3]Department of Chemistry, University of Illinois at Chicago, Chicago, IL 60607, USA. [4]Department of Biochemistry and Molecular Biology, University of Oklahoma Health Sciences Center, Oklahoma City, OK 73104, USA.

*To whom correspondence should be addressed. E-mail: jordan-tang@omrf.ouhsc.edu

2 is a class I transmembrane protein consisting of an NH_2-terminal protease domain, a connecting strand, a transmembrane region, and a cytosolic domain (*6, 7*). Sequence homology with other aspartic proteases suggests that memapsin 2 has a pro sequence of about 48 residues at its NH_2-terminal region. The protease domain of pro-memapsin 2, expressed recombinantly, hydrolyzes peptides from the APP β-secretase site but has a broad specificity (*6*). We have used this specificity information to design potent inhibitors against this enzyme (*8*). OM99-2, an eight-residue transition-state inhibitor (Fig. 1) has a K_i of 1.6 nM for memapsin 2. To develop memapsin 2 inhibitors with therapeutic potential would require, besides good potency and pharmacokinetic properties, low molecular weight (<700 daltons) and high lipophilicity in order to penetrate the blood-brain barrier (*9*). We determined the three-dimensional structure of the memapsin 2 with an active site–bound OM99-2 at 1.9 Å resolution in order to define a template for the rational design of memapsin 2 inhibitor drugs.

Fully active recombinant memapsin 2, which contains 21 residues of the putative pro region, residues numbers 28p–48p (*10*) but without the transmembrane and intracellular domains (*11*), was crystallized as a complex with OM99-2 (*12*). We report here a crystal structure of this complex at 1.9 Å resolution. The crystal structure was determined using molecular replacement methods (*12*) with human pepsin (22% sequence identity) as the search model. The statistical data are shown in Table 1.

The bilobal structure of memapsin 2 (Fig. 2A) has the conserved general folding of aspartic proteases (*13*). The inhibitor is located in the substrate binding cleft between the NH_2- and COOH-terminal lobes (*10*) (Fig. 2A). Active-site Asp^{32} and Asp^{228} and the surrounding hydrogen bond network are located in the center of the cleft (Fig. 2, A and B) and are conserved (*14*). The hairpin loop known as the "flap" (*10*) partially covers the cleft. The active-site carboxyls are, however, not co-planar, and the degree of deviation (50°) exceeds those observed previously. Whether this is specific for OM99-2 binding has not been determined.

Compared to pepsin (*15*), the most significant structural differences are the insertions and a COOH-terminal extension in the C-lobe. Four insertions, A, C, D, and F (*10*) (Fig. 2, A and B), as helices and loops are located on the adjacent molecular surface near the NH_2-terminus of the inhibitor. Insertion F (*10*), which contains four acidic residues, forms the most negatively charged region on the molecular surface. Together, these insertions significantly enlarge the molecular boundary of memapsin 2 as compared to pepsin (Fig. 2B). These surface structural changes may function in the association of memapsin 2 with other cell-surface components. Insertions B and E are located on the molecular surface near the COOH-terminus of the inhibitor. Loop E is connected to a β-strand that is paired with part of the COOH-terminal extension. The active-site cleft of memapsin 2 is, in general, more open and accessible than that of pepsin, owing to structural differences near respective subsites P_4, P_2, and P_1' (see below) and the absence of six pepsin residues [P^{292}TESGE^{297} (*16*)] at memapsin 2 residues Thr^{329}/Gly^{330} on a loop opposite the flap across the active-site cleft. The 35-residue COOH-terminal extension (*10*) unique to memapsin 2 consists mostly of highly ordered structure (residues 359–385). Residues 369–376 form a β structure with seven hydrogen bonds to strand 293–299, whereas residues 378–383 form a helix (Fig. 2A).

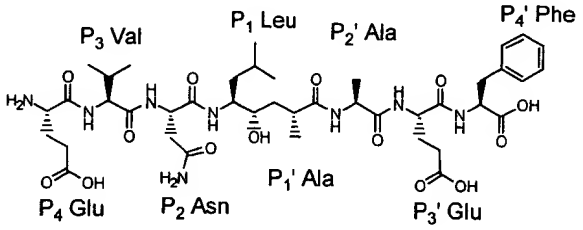

Fig. 1. The chemical structure of memapsin 2 inhibitor OM99-2 with the constituent amino acids and their subsite designations. The hydroxyethylene transition-state isostere is between P_1-Leu and P_1'-Ala.

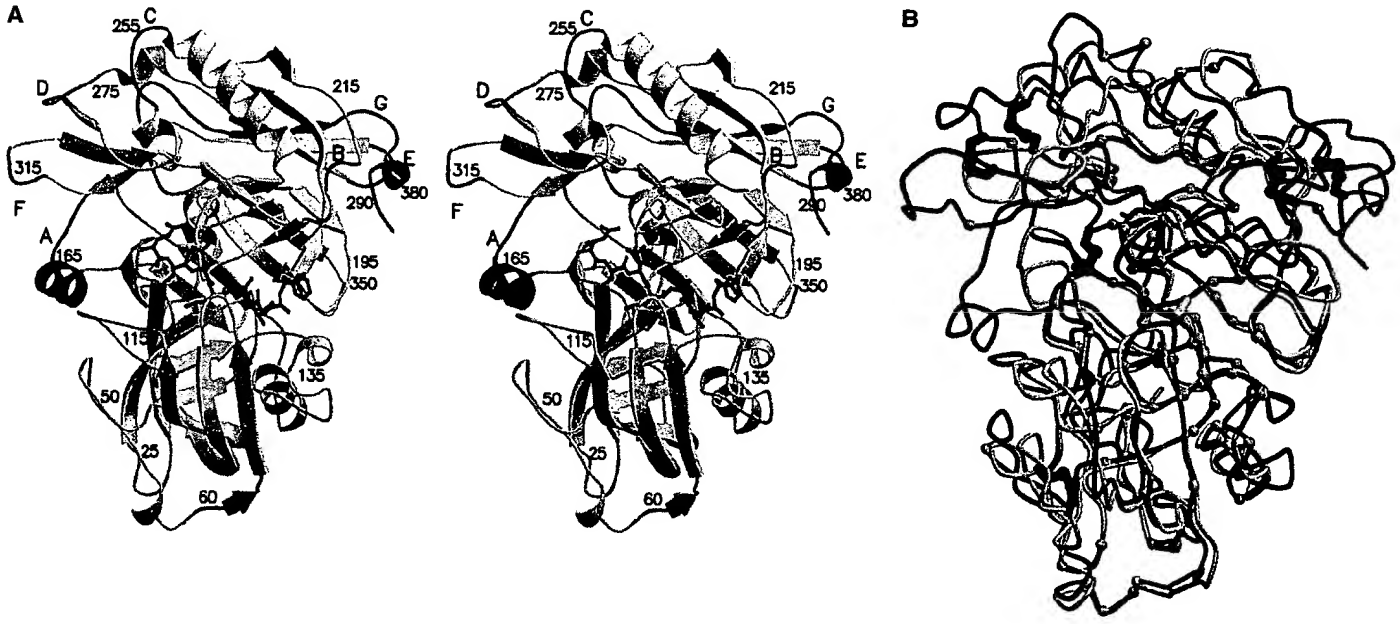

Fig. 2. The crystal structure of memapsin 2 complexed to inhibitor OM99-2. (**A**) Stereo view of the polypeptide backbone of memapsin 2 is shown as a ribbon diagram. The N-lobe and C-lobe are blue and yellow, respectively, except the insertion loops, designated A to G (*10*) in the C-lobe are magenta and the COOH-terminal extension is green. The inhibitor bound between the lobes is shown in red. (**B**) The chain tracing of human memapsin 2 (dark blue) and human pepsin (gray) is compared. The light blue balls represent identical residues which are topologically equivalent. The disulfide bonds are shown in red for memapsin 2 and orange for pepsin. The COOH-terminal extension is in green. The active-site aspartic acids are shown in yellow.

Two of the three disulfide pairs (residues 155 and 359 and 217 and 382) unique to memapsin 2 fasten both ends of the extension region to the C-lobe. This COOH-terminal extension is longer than those observed previously for aspartic proteases and is conformationally quite different (*17–20*). The last eight residues (386–393) are not seen in the electron density map. Their mobility suggests the possibility of forming a short stem between the globular catalytic domain and the trans-membrane domain. Of the 21 putative pro residues present in the enzyme (*10*), only the last six, 43p–48p, are visible in the electron density map. The others are likely mobile, which is consistent with an unstructured pro segment being displaced from the active-site cleft by the inhibitor (*21*).

The interactions of the eight-residue inhibitor OM99-2 with memapsin 2 include four hydrogen bonds between two active-site aspartates and the hydroxyl of the transition-state isostere, and ten hydrogen bonds from different parts of the binding cleft and flap to inhibitor backbone (Fig. 3). Most of these hydrogen bonds are highly conserved among eukaryotic (*14, 22, 23*) and HIV (*24*) aspartic proteases, except hydrogen bonds to Gly^{11} and Tyr^{198}. The protease residues in contact with individual inhibitor side chains (Fig. 3) are, however, quite different compared with other aspartic proteases (especially at S_3, S_1, and S_1'). Some of these differences can be traced to various insertions and deletions around the cleft. Five NH_2-terminal residues of OM99-2 are in an extended conformation and, with the exception of P_1'-Ala, all have clear contacts (within 4 Å) which define protease subsites (Fig. 3). The protease S_4 subsite is mostly hydrophilic and open to solvent. The inhibitor P_4-Glu side chain is hydrogen bonded to P_2-Asn and is also close to the Arg^{235} and Arg^{307} side chains (Fig. 3), which may explain why deleting this residue from OM99-2, to give the shorter inhibitor OM99-1, causes a 10-fold increase in K_i (*8, 25*). The protease S_2 subsite is also relatively hydrophilic and open to solvent. The hydrophilic character of the memapsin 2 S_4 and S_2 subsites is not conserved in the corresponding subsites of human aspartic proteases, such as pepsin, gastricsin, and cathepsins D and E. This difference may be utilized to design selectivity into memapsin 2 inhibitors. The relatively small S_2 residues Ser^{325} and Ser^{327} (Gln and Met, respectively, in pepsin) may accommodate an inhibitor side chain larger than P_2-Asn. The memapsin 2 S_1 and S_3 subsites, consisting mostly of hydrophobic residues, have conformations very different from pepsin due to the absence of a pepsin helix at residues 111–114 (*26, 27*). The

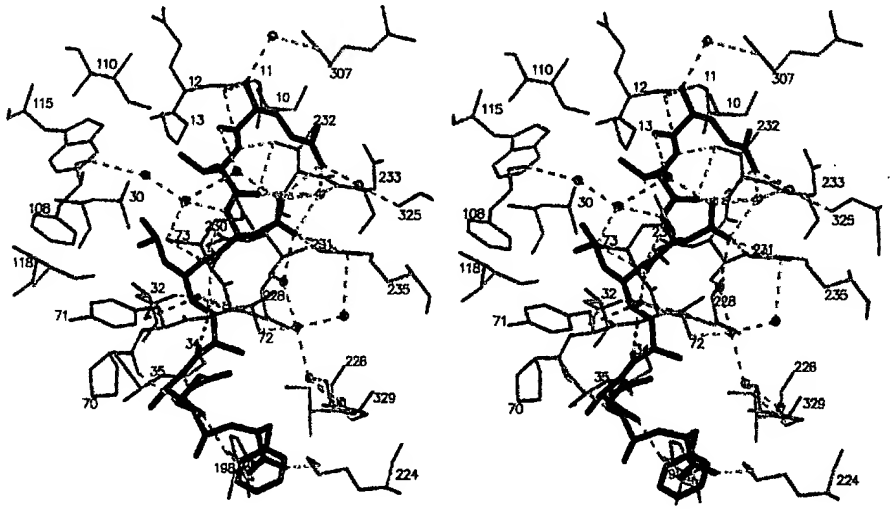

Fig. 3. Stereo presentation of interactions between inhibitor OM99-2 (orange) and memapsin 2 (light blue). Nitrogen and oxygen atoms are marked blue and red, respectively. Hydrogen bonds are indicated in yellow dotted lines. Memapsin 2 residues which comprise the binding subsites are included.

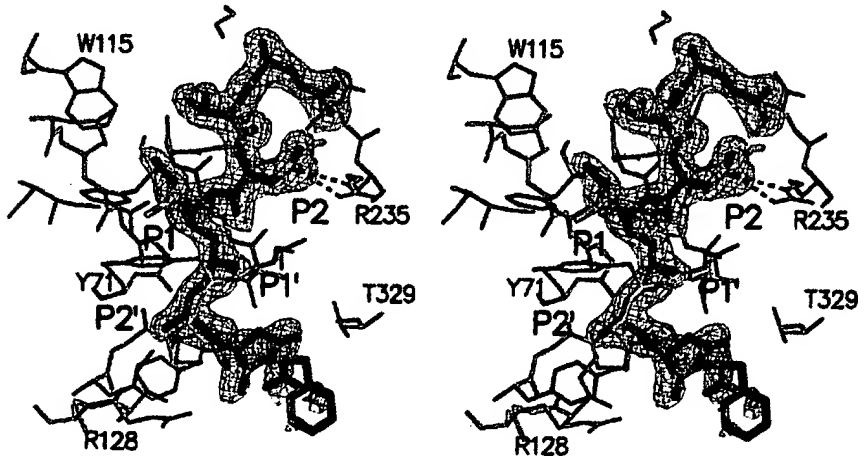

Fig. 4. Electron density of inhibitor OM99-2 and the differences in the binding of Swedish and native APP at P_1 and P_2.The omit electron density map (the $|F_o| - |F_c|$ map with the inhibitor excluded from the phase calculation), contoured at 2 σ, is superimposed onto the inhibitor model with carbon atoms in green, nitrogen atoms in blue, and oxygen atoms in red. Asn and Leu side chains are those for the Swedish mutant APP at P_2 and P_1, respectively. The hydrogen bonds between inhibitor P_2 residue Asn and Arg^{235} are shown in magenta. The side chains of Lys and Met (in yellow) are those for the wild-type APP, and are modeled for comparison. The turn of the inhibitor backbone at P_2' is clearly visible.

Table 1. Data collection and refinement statistics.

Data statistics	
Space group	$P2_1$
Unit cell a, b, and c (Å)	53.7, 85.9, 109.2
α, β, and γ (degrees)	90.0, 101.4, 90.0
Resolution (Å)	25.0–1.9
Number of observed reflections	144,164
Number of unique reflections	69,056
R_{merge}*	0.061 (0.25)
Data completeness (%) (25.0–1.9 Å)	90.0 (68.5)
$\langle I/\sigma(I)\rangle$	13.7 (3.0)
Refinement statistics	
$R_{working}$†	0.180
R_{free}†	0.224
RMS deviation from ideal values	
Bond length (Å)	0.014
Bond angle (degrees)	1.8
Number of water molecules	529
Average *B* factor (Å²)	
Protein	28.3
Solvent	34.0

*$R_{merge} = \Sigma_{hkl} \Sigma_i |I_{hkl,i} - \langle I_{hkl}\rangle| / \Sigma_{hkl} \langle I_{hkl}\rangle$, where $I_{hkl,i}$ is the intensity of the *i*th measurement and $\langle I_{hkl}\rangle$ is the weighted mean of all measurements of I_{hkl}. †$R_{working}$ (and R_{free}) $= \Sigma||F_o| - |F_c|| / \Sigma|F_o|$, where F_o and F_c are the observed and calculated structure factors. Numbers in parentheses are the corresponding numbers for the highest resolution shell (2.00–1.9 Å). Reflections with $F_o/\sigma(F_o) \geq 0.0$ are included in the refinement and *R* factor calculation.

inhibitor side chains of P_3-Val and P_1-Leu are closely packed against each other and have substantial hydrophobic contacts with the enzyme (Fig. 3), especially P_1, which interacts with Tyr^{71} and Phe^{108}. In native APP, the P_2 and P_1 residues adjacent to the β-secretase cleavage site are Lys and Met, respectively. Swedish mutant APP has Asn and Leu in these positions, resulting in a 60-fold increase of k_{cat}/K_m over that of the native APP (*6*) and an early onset of AD (*28*). The inhibitor P_2-Asn side chain has hydrogen bonds to P_4 Glu and Arg^{235} (Figs. 3 and 4). Replacing P_2-Asn with Lys would result in the loss of these hydrogen bonds and the positive charge would likely interact unfavorably with the Arg^{235} side chain. P_1-Met would also likely have less favorable contact with the enzyme than P_1-Leu (Fig. 4). No close contact with memapsin 2 was seen for P_1'-Ala. An aspartic acid at this position, as in native APP, may be accommodated.

The direction of inhibitor chain turns at P_2' and leads P_3' and P_4' toward the protein surface (Figs. 3 and 4). As a result, the backbone of these three inhibitor residues deviates from the regular extended conformation. The side chains of P_3'-Glu and P_4'-Phe point toward the molecular surface, but have little interaction with the protease, while the terminal COOH group of P_4' has a salt bridge to Lys^{224} and hydrogen bonded to the hydroxyl group of Tyr^{198}. These two COOH-terminal residues have relatively high average *B* factors (56.7 Å^2 for P_3'-Glu and 71.9 Å^2 for P_4'-Phe as compared to 27.4, 22.6, 21.5, 23.7, 24.7, and 29.7 Å^2 for residues P_4–P_2', respectively) and poorly defined electron density, suggesting that they are relatively mobile. In contrast, the S_3' and S_4' subsites in renin-inhibitor (CH-66) complex (*23*) have a defined structure. The topologically equivalent region of these renin subsites (residues 293–298 in pepsin numbering) is absent in memapsin 2. The conformation of P_2' to P_4', including a kink at P_2' and the change of backbone direction at P_3' and P_4', is rare in aspartic protease inhbitors. The backbone turn at P_2' is likely caused by a hydrogen bond between P_2' carbonyl and hydroxyl of Tyr^{198}, not seen in the inhibitor complexes of renin (*23*) and endothiapepsin (*22*). A similar hydrogen bond is present in pepsin and a similar P_2' kink has been observed for one of its inhibitors (*27*). The conformation of the three COOH-terminal residues of OM99-2, including the kink at the P_2' backbone, may be a way to direct a long protein substrate out of the active-site cleft.

The well-defined subsite structures spanning P_4 to P_2' provide a template for rational design of drugs against memapsin 2. The unusual conformation of subsites P_2', P_3', and P_4' may facilitate the design of inhibitors selective for memapsin 2.

References and Notes

1. D. J. Selkoe, *Nature* **399A**, 23 (1999).
2. M. S. Wolfe *et al.*, *Nature* **398**, 513 (1999).
3. Y.M. Li *et al.*, *Nature* **405**, 689 (2000).
4. W. P. Esler *et al.*, *Nature Cell Biol.* **2**, 428 (2000).
5. S. Sinha and I. Lieberburg, *Proc. Natl. Acad. Sci. U.S.A.* **96**, 11049 (1999).
6. X. Lin *et al.*, *Proc. Natl. Acad. Sci. U.S.A.* **97**, 1456 (2000).
7. β-Secretase was reported as, besides memapsin 2 (*6*), also (i) BACE [R. Vassar *et al.*, *Science* **286**, 735 (1999)], (ii) Asp 2 [R. Yan *et al.*, *Nature* **402**, 533 (1999)], (iii) membrane-bound aspartic proteinase [S. Sinha *et al.*, *Nature* **402**, 537 (1999)], and (iv) Asp 2 [I. Hussain *et al.*, *Mol. Cell. Neurosci.* **14**, 419 (1999)].
8. OM99-2 is based on an octapeptide sequence of Glu-Val-Asn-Leu-Ala-Ala-Glu-Phe in which the Leu-Ala bond is substituted by a hydroxyethylene transition-state isostere (*25*). The K_i value reported for recombinant pro-memapsin 2 (*6*) was 9.8 nM (*25*). The K_i value for recombinant memapsin 2 used in this structural study has been determined to be 1.6 nM (*21*).
9. B. P. Kearney and F. T. Aweeka, *Neurol. Clin.* **17**, 883 (1999).
10. The putative pro residues 28p–48p present in memapsin 2 used for structural determination are LRLPRETDEEPEEPGRRGSFV. The alignment of amino acid sequences and secondary structures of memapin 2 and human pepsin is shown in an additional Web figure (*29*). The numbering of residues in memapsin 2 used in this paper starts at Glu^1 in the sequence of EMVDN- and continues based on the published memapsin 2 sequence (*6*). The positions and marker sequences of the regions discussed in the text (insertions A through G) are: NH_2-terminal lobe, residues 1–180, starting at Glu^1 to the end of sequence IGGID^{180}; COOH-terminal lobe, residues 181–385, starting at His^{181} in the sequence of HSLYT to the end of COOH-terminal extension G (see below); flap residues, VPYTQGK (residues 69–75); insertion A, GFPLNQSEVL (residues 158–167); insertion B, KEYN (residues 218–221); insertion C, ASSTEKFP (residues 251–258); insertion D, WQAG (residues 270–273); insertion E, EVTNQS (residues 290–295); insertion F, DVATSQD (residues 311–317); and COOH-terminal extension G, CHVHDEFRTAAVEGPFVTLDMEDCGYNIPQTDEST (residues 359–393).
11. Residues 1p to 393 of human pro-memapsin 2 [residues 28p to 393 are shown in additional Web figure (*29*); the complete pro sequence is described in (*6*)] was expressed from vector pET11a using an *Escherichia coli* host BL21(DE3) as previously described (*6*). The inclusion bodies were harvested, washed, and dissolved in 0.1 M tris, 1 mM EDTA, 1 mM glycine, 8 M urea, and 0.1 M β-mercaptoethanol (pH 10), and then refolded by rapid dilution as previously described (*30*). The recombinant pro-memapsin 2 was purified by gel filtration on Sepharose S-300 and FPLC on Resource-Q (Pharmacia) column (*30*). The NH_2-terminal sequence of purified memapsin 2 established that it started at Leu^{28p} with a minor component starting at Leu^{30p}. Since the expressed pro-memapsin 2 had been determined to contain 48 putative pro residues [starting at the sequence of Ala-Gly-Val-Leu- (*6*)], activation with the removal of part of the pro peptide (residues 1p to 28p or 30p) had taken place during the preparation procedure. This purified enzyme form has the highest specific activity [using the assay described in (*25*); see also (*6*)] among all the activated memapsin 2 (*21*).
12. Purified recombinant memapsin 2 in the presence of fivefold molar excess of OM99-2 was crystallized in 0.2 M ammonium sulfate and 22.5% PEG 8000 buffered with 0.1 M Na-cacodylate (pH 7.4) at 20°C, using the hanging drop vapor diffusion method. The typical crystal size was about 0.4 mm by 0.4 mm by 0.2 mm. Diffraction data were collected at 95 K with an Raxis-IV image plate, integrated and reduced with the HKL program package [Z. Otwinowski and W. Minor, *Methods Enzymol.* **276**, 307 (1997)]. The crystals belong to the space group $P2_1$ with two memapsin 2/OM99-2 complexes per crystallographic asymmetric unit and 56% solvent content. The molecular replacement calculations were performed using pepsin (Protein Data Bank accession number 1psn) as the search model with the program AMoRe [J. Navaza, *Acta Crystallogr. A* **50**, 157 (1994)]. The refinement was carried out using the program CNS (*31*)]. The molecular graphic program O [T. A. Jones, J. Y. Zou, S. W. Cowan, M. Kjelgaard, *Acta Crystallogr. A* **47**, 110 (1991)] was used for interactive map fitting. The initial solution had a correlation coefficient of 22% and an *R* factor of 0.51 for data in the range of 15 to 3.5 Å. The $|F_o| - |F_c|$ omit map from early stages of refinement revealed surplus electron density within the active-site cleft, which was fitted with the inhibitor structure. After multiple cycles of refinement and model building, the $R_{working}$ and R_{free} values of the final structure were 18.0 and 22.4%, respectively. Crystallographic refinement used molecular dynamics and energy minimization functions of CNS (*31*). No solvent molecules were added to the model until the *R* factor was reduced below 0.25. Solvent molecules, 529, were then added as identified in the $|F_o| - |F_c|$ map contoured at the 3 σ level. Noncrystallographic symmetry restriction and averaging were used in early stages of refinement and model building. Bulk solvent and anisotropic overall *B* factor corrections were applied through the refinement. In the final model, no backbone φ, ψ torsion angles were located in the disallowed region of the Ramachandran plot whereas 90% of the residues were located in the most favored regions, as defined by the program PROCHECK [R. A. Laskowski, M. W. MacArthur, D. S. Moss, J. M. Thornton. *J. Appl. Crystallogr.* **26**, 283 (1993)]. The two memapsin 2/OM99-2 complexes in the crystallographic asymmetric unit are essentially identical.
13. J. Tang, M. N. James, I. N. Hsu, J. A. Jenkins, T. L. Blundell, *Nature* **271**, 618 (1978).
14. D. R. Davies, *Annu. Rev. Biophys. Biophys. Chem.* **19**, 189 (1990).
15. A. R. Seileki, A. A. Fedorov, A. Boodhoo, N. S. Andreeva, M. N. James, *J. Mol. Biol.* **214**, 143 (1990).
16. Single-letter abbreviations for the amino acid residues are as follows: A, Ala; C, Cys; D, Asp; E, Glu; F, Phe; G, Gly; H, His; I, Ile; K, Lys; L, Leu; M, Met; N, Asn; P, Pro; Q, Gln; R, Arg; S, Ser; T, Thr; V, Val; W, Trp; and Y, Tyr.
17. S. M. Cutfield *et al.*, *Structure* **3**, 1261 (1995).
18. C. Abad-Zapatero *et al.*, *Protein Sci.* **5**, 640 (1996).
19. J. Symersky, M. Monod, S. I. Foundling, *Biochemistry* **36**, 12700 (1997).
20. J. Yang and J. W. Quail, *Acta Crystallogr. D* **55**, 625 (1999).
21. J. Ermolieff, J. A. Loy, G. Koelsch, J. Tang, *Biochemistry*, in press.
22. D. Bailey and J. B. Cooper, *Protein Sci.* **3**, 3129 (1994).
23. C. G. Dealwis *et al.*, *J. Mol. Biol.* **236**, 342 (1994).
24. A. Wlodawer and J. W. Erickson, *Annu. Rev. Biochem.* **62**, 343 (1993).
25. A. Ghosh *et al.*, *J. Am. Chem. Soc.* **122**, 3522 (2000).
26. M. Fujinaga, M. M. Chernaia, N. I. Tarasova, S. C. Mosimann, M. N. James, *Protein Sci.* **4**, 960 (1995).
27. M. Fujinaga *et al.*, *Acta Crystallogr. D* **56**, 272 (2000).
28. M. Mullan *et al.*, *Nature Genet.* **2**, 340 (1992).
29. Supplementary Web figure is available at www.sciencemag.org/feature/data/1052536.shl.
30. X. Lin, Y. Lin, J. Tang, *Methods Enzymol.* **241**, 195 (1994).
31. A. T. Brünger *et al.*, *Acta Crystallogr. D* **54**, 905 (1998).

32. We thank D. R. Davies, A. Wlodawer, and J. D. Capra for critical reading of this manuscript, and D. Downs and A. Irwin for assisting in enzyme preparation. Coordinates have been deposited in the Protein Data Bank (accession number 1FKN). J.T. is holder of the J. G. Puterbaugh Chair in Biomedical Research at the Oklahoma Medical Research Foundation. G.K. is a Scientist Development Awardee of the American Heart Association.

24 May 2000; accepted 17 August 2000

United States Patent Application **20020115600**
Kind Code **A1**
Koelsch, Gerald ; et al. **August 22, 2002**

Inhibitors of ***memapsin 2*** and use thereof

Abstract

Methods for the production of purified, catalytically active, recombinant ***memapsin 2*** have been developed. The substrate and subsite specificity of the catalytically active enzyme have been determined. The substrate and subsite specificity information was used to design substrate analogs of the natural ***memapsin 2*** substrate that can inhibit the function of ***memapsin 2***. The substrate analogs are based on peptide sequences, shown to be related to the natural peptide substrates for ***memapsin 2***. The substrate analogs contain at least one analog of an amide bond which is not capable of being cleaved by ***memapsin 2***. Processes for the synthesis of two substrate analogues including isosteres at the sites of the critical amino acid residues were developed and the substrate analogues, OMR99-1 and OM99-2, were synthesized. OM99-2 is based on an octapeptide Glu-Val-Asn-Leu-Ala-Ala-Glu-Phe (SEQ ID NO:28) with the Leu-Ala peptide bond substituted by a transition-state isostere hydroxyethylene group (FIG. 1). The inhibition constant of OM99-2 is 1.6.times.10.sup.-9 M against recombinant pro-***memapsin 2***. Crystallography of ***memapsin 2*** bound to this inhibitor was used to determine the tliree dimensional structure of the protein, as well as the importance of the various residues in binding. This information can be used by those skilled in the art to design new inhibitors, using commercially available software programs and techniques familiar to those in organic chemistry and enzymology, to design new inhibitors to ***memapsin 2,*** useful in diagnostics and for the treatment and/or prevention of Alzheimer's disease.

Inventors: **Koelsch, Gerald**; *(Oklahoma City, OK)* ; **Tang, Jordan J.N.**; *(Edmond, OK)* ; **Hong, Lin**; *(Oklahoma City, OK)* ; **Ghosh, Arun K.**; *(River Forest, IL)*

Correspondence Name and Address:
Patrea L. Pabst
Arnall Golden & Gregory, LLP
2800 One Atlantic Center
1201 West Peachtree Street
Atlanta
GA
30309-3450
US

Assignee Name and Adress: **Oklahoma Medical Research Foundation**
Serial No.: **845226**
Series Code: **09**
Filed: **April 30, 2001**

U.S. Current Class:	**514/12**; 435/184; 530/326
U.S. Class at Publication:	**514/12**; 435/184; 530/326
Intern'l Class:	A61K 038/17; A61K 038/00

Claims

We claim:

1. An inhibitor of catalytically active ***memapsin 2*** which binds to the active site of the ***memapsin 2*** defined by the presence of two catalytic aspartic residues and substrate binding cleft.

2. The inhibitor of claim 1 comprising an isostere of the active site of ***memapsin 2***.

3. The inhibitor of claim 2 comprising a molecule having the general form X- L.sub.4-P.sub.4-L.sub.3-P.sub.3-L.sub.2-P.sub.2-L.sub.1-P.sub.1-L.sub.- 0-P.sub.1'-L.sub.1'-P.sub.2'-L.sub.2'-P.sub.3'-L.sub.3'-P.sub.4'L.sub.4'-Y- , wherein Px represent the substrate specificity position relative to the cleavage site which is represented by an -LO-, and Lx represent the linking regions between each substrate specificity position, Px, and wherein L.sub.0 is a non-hydrolyzable bond and P1'is -R.sub.1CR.sub.3-, wherein R.sub.1 is a group smaller than CH.sub.2OH (side chain of serine), and at least two other P positions are a hydrophobic group.

4. The inhibitor of claim 3 which is OM99-1.

5. The inhibitor of claim 3 which is OM99-2.

6. The inhibitor of claim 3 having the structure of FIG. 11.

7. The inhibitor of claim 3 having the structure of FIG. 12.

8. The inhibitor of claim 3 having the structure of FIG. 13.

9. The inhibitor of claim 3 having the structure of FIG. 14.

10. The inhibitor of claim 1 having an K.sub.i of less than or equal to 10.sup.-7 M.

11. The inhibitor of claim I which binds to crystallized enzyme characterized by the parameters in Table 2 when bound to OM-99-2.

12. The inhibitor of claim 13 having a K.sub.i of less than or equal to 10.sup.-6 M.

13. The inhibitor of claim 11 having a K.sub.i of less than or equal to 2 nM.

United States Patent Application **20020049303**
Kind Code **A1**
Tang, Jordan J. N. ; et al. **April 25, 2002**

Catalytically active recombinant memapsin and methods of use thereof

Abstract

Methods for the production of purified, catalytically active, recombinant ***memapsin 2*** have been developed. The substrate and subsite specificity of the catalytically active enzyme have been determined. The substrate and subsite specificity information was used to design substrate analogs of the natural ***memapsin 2*** substrate that can inhibit the function of ***memapsin 2***. The substrate analogs are based on peptide sequences, shown to be related to the natural peptide substrates for ***memapsin 2***. The substrate analogs contain at least one analog of an amide bond which is not capable of being cleaved by ***memapsin 2***. Processes for the synthesis of two substrate analogs including isosteres at the sites of the critical amino acid residues were developed and the substrate analogs, OMR99-1 and OM99-2, were synthesized. OM99-2 is based on an octapeptide Glu-Val-Asn-Leu-Ala-Ala-Glu-Phe (SEQ ID NO:28) with the Leu-Ala peptide bond substituted by a transition-state isostere hydroxyethylene group (FIG. 1). The inhibition constant of OM99-2 is 1.6.times.10.sup.-9 M against recombinant pro-***memapsin 2***. Crystallography of ***memapsin 2*** bound to this inhibitor was used to determine the three dimensional structure of the protein, as well as the importance of the various residues in binding. This information can be used by those skilled in the art to design new inhibitors, using commercially available software programs and techniques familiar to those in organic chemistry and enzymology, to design new inhibitors to ***memapsin 2,*** useful in diagnostics and for the treatment and/or prevention of Alzheimer's disease.

Inventors: **Tang, Jordan J. N.**; *(Edmond, OK)* ; **Lin, Xinli**; *(Edmond, OK)* ; **Koelsch, Gerald**; *(Oklahoma City, OK)* ; **Hong, Lin**; *(Oklahoma City, OK)*

Correspondence Name and Address:
PATREA L. PABST
HOLLAND & KNIGHT LLP
SUITE 2000, ONE ATLANTIC CENTER
1201 WEST PEACHTREE STREET, N.E.
ATLANTA
GA
30309-3400
US

Serial No.: **796264**
Series Code: **09**
Filed: **February 28, 2001**

U.S. Current Class:	**530/350**; 435/252.3; 435/320.1; 435/6; 435/69.1; 435/69.2; 530/387.9
U.S. Class at Publication:	**530/350**; 435/69.1; 435/252.3; 435/320.1; 435/6; 435/69.2; 514/2; 530/387.9
Intern'l Class:	C12N 015/09; C12N 009/64; C12N 015/74

Claims

We claim:

1. Purified recombinant catalytically active ***memapsin 2***.

2. The ***memapsin 2*** of claim 1 having the amino acid sequence of SEQ ID NO.2 or the sequence present in a homologous species.

3. The ***memapsin 2*** of cliam 2 of human origin and having the amino acid sequence of SEQ ID NO.2.

4. The ***memapsin 2*** of claim 1 not including the transmembrane domain.

5. The ***memapsin 2*** of claim 1 expressed in a bacteria.

6. The ***memapsin 2*** of claim 1 cleaving SEVKM/DAEFR (SEQ ID NO:4) and SEVNL/DAEFR (SEQ ID NO:5) at pH 4.0 with k.sub.cat/K.sub.m of less than or equal to 39.9 s.sup.-1M.sup.-1 and less than or equal to k.sub.cat, 2.45 s.sup.-1, K.sub.m, 1 mM; k.sub.cat/K.sub.m, 2450 s.sup.-1M.sup.-1, respectively.

7. A method for producing catalytically active recombinant ***memapsin 2*** comprising refolding the recombinant ***memapsin 2*** under conditions which dissociate and then slowly refold the enzyme into a catalytically active form.

8. The method of claim 7 wherein the ***memapsin 2*** is first dissolved in 8 M urea solution including one or more reducing agents at a pH of greater than 8.0.

9. The method of claim 8 wherein the ***memapsin 2*** is then diluted into an aqueous buffer like 20 mM-Tris, pH 9.0, the pH slowly adjusted to approximately 8 with 1 M HCl, and the solution maintained at low temperature for approximately 24 to 48 hours before proceeding with purification.

10. The method of claim 8 wherein the ***memapsin 2*** is then rapidly mixed with an aqueous buffer like 20 mM-Tris, pH 9.0, containing oxidized and reduced glutathione, the process repeated, then the urea concentration decreased to approximately 0.4 M and the pH of the solution slowly adjusted to 8.0.

11. The method of claim 8 wherein the ***memapsin 2*** is dissolved in 8 M urea, pH 10.0, then rapidly diluted into an aqueous buffer like 20 mM Tris base, pH 9.0, and maintained at low temperature several